C-8-3 RAIN ATTENUATION CHARACTERISTICS ON EARTH-SPACE LINKS

Kohhei SATOH Yoshio HOSOYA
Yokosuka Electrical Communication Laboratory,
Nippon Telegraph and Telephone Public Corporation,
Yokosuka-shi, Kanagawa-ken, Japan

1. Introduction

In designing satellite communication systems using frequencies above 10 GHz, the slant path rain attenuation is one of significant factors to be taken into consideration. Extensive measurements had been made by using sun-tracking radiometers, passive radiometers and so on.[1] Site diversity is a very promising technique to overcome excessive rain attenuation. The results of site diversity effect measurement are also reported.[1] However, the prediction method used for rain attenuation and site diversity effects, which is applicable to districts where no measured results are available, has been scarcely established.

At Electrical Communication Laboratories (ECL), N.T.T., slant path rain attenuation has been measured since 1969, together with statistical analysis based on meteorological data. In the first-phase experiment conducted from 1969 to 1973, the rain attenuation and site diversity effects had been measured by using 11 and 18 GHz sun-tracking radiometer set at Musashino ECL and 18 GHz passive radiometer at Shibuya. The rain rates had been measured by rain-gauges set out around two sites. Research to derive the statistical prediction method for estimating rain attenuation distribution and site diversity effects has also been accomplished along with the experiment. As the result of these experimental and theoretical studies, it was found that the rain attenuation and site diversity effects could be estimated by means of surface rain rate distribution, rain rate spatial correlation and so on. It was confirmed that calculated values agreed well with measured values.[2] Since 1975, experiments have been continued at Yokosuka ECL and Kawasaki, southwest of Tokyo. The 17 and 27 GHz sun-tracking radiometer is set at Yokosuka ECL and the 18 GHz passive radiometer, fixed at 20° and 55° elevation angles, is set at Kawasaki. The second-phase experiment is different from the first-phase experiment in location, weather conditions, frequencies and diversity distance.

This paper describes results obtained in this second-phase experiment from 1975 to 1977. It was confirmed that the above-mentioned prediction method could be applicable to other conditions which differ from the first-phase experiment in frequencies, diversity distance and so on.

2. Measurements outline

Figure 1 shows an area map of the second-phase experiment. The 17 and 27 GHz sun-tracking radiometer is located at Yokosuka ECL and has two antennas, one of which is directed at the sun and the other at the sky about 2.5° away. The 18 GHz passive radiometer is set up at Kawasaki, 33 km from Yokosuka ECL. It has two antennas, one of which is fixed at 20° elevation angle and the other at 55° elevation angle. The azimuth of the antenna beams is 216°, as shown in Fig.1. Dynamic range of sun-tracking and passive radiometers are 25 dB and 10 dB, respectively. A network of tipping-bucket rain-gauges is installed in Yokosuka and Kawasaki areas. The minimum detectable rain rate is 3.0 mm/h for an integration time of 1 minute. Observation period is about 2.5 years, from March 1975 to August 1977.

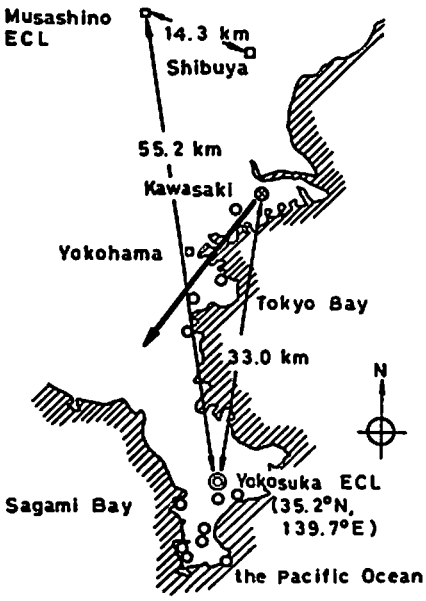

◉ : 17 and 27 GHZ sun-tracking radiometer
⊗ : 18 GHZ passive radiometer
○ : Rain-gauge

Fig.1 Experimental area map

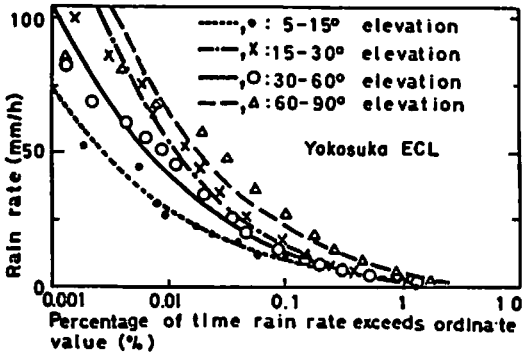

Fig.2 Cumulative distribution of point rain rate at Yokosuka ECL

Table 1 Rain rate distribution parameters

Elevation angle	m	σ^2
5° - 15°	-0.5255	0.4170
15° - 30°	-0.3406	0.4081
30°- 60°	-0.5514	0.5501
60°- 90°	-0.0181	0.3511

3. Measurement results and considerations

3.1 Rain rate distribution

Figure 2 shows measured cumulative distribution of surface point rain rate at Yokosuka ECL. For the theoretical calculation of rain attenuation, it is necessary to obtain the rain rate distribution function. When probability distri-

bution function of rain rate R(mm/h) is approximated by the log-normal distribution, probability density function f(R) can be given by;

$$f(R)=\frac{K}{\sqrt{2\pi}R\sigma}\exp\{-\frac{(\log R-m)^2}{2\sigma^2}\},\quad 0<R<\infty \qquad (1)$$

where, K=log e, and m and σ^2 are average value and variance in logR distribution, respectively.

The curves in Fig.2 show theoretical values of the log-normal distribution, which agree best with the measured values, respectively. Table 1 shows m and σ^2 values. As shown in this figure, the log-normal distribution curves give good approximation to measured values for 0.01% of the time or more, around which the satellite circuit availability is usually considered.

3.2 Rain attenuation distribution

Rain attenuation distribution at 17 and 27 GHz are shown in Figs.3-a and 3-b, respectively. A method for calculating rain attenuation distribution was proposed by Morita and Higuti,[2] which was obtained from an analysis of the first-phase experiment. In that paper, it is assumed that rain attenuation occurs below the 0°C layer height. The rain attenuation distribution can be estimated by using average 0°C layer height obtained by aerological observations, rain rate distribution, rain rate spatial correlation, specific rain attenuation and elevation angle.

The slant path rain attenuation distribution at Yokosuka ECL is calculated by using the above-mentioned method and by assuming the following parameter.

(a) Point rain rate distribution given in Fig.2 and Table 1 is used.

(b) Rain rate spatial correlation

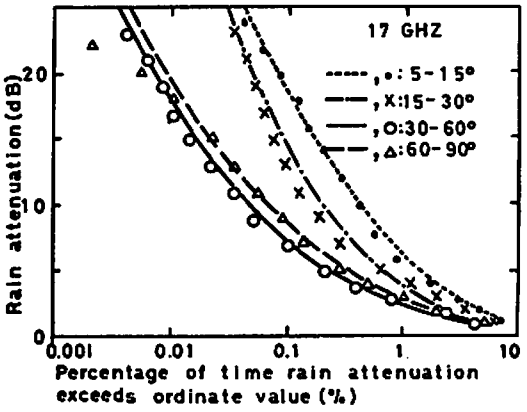

Fig.3-a Comparison of measured and calculated cumulative rain attenuation distribution at 17 GHz

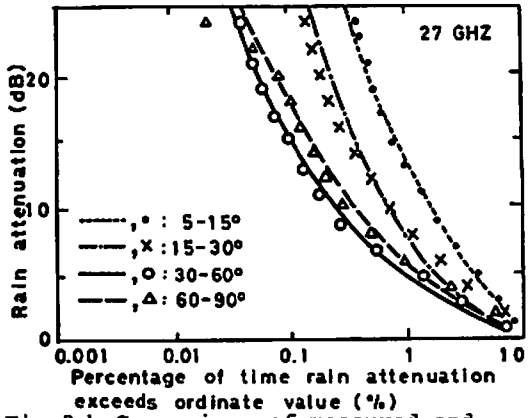

Fig.3-b Comparison of measured and calculated cumulative rain attenuation distribution at 27 GHz

function ρ is $\rho = \exp(-0.35\sqrt{d})$, where d(km) is distance.(2)

(c) Equivalent rain layer height is average 0°C layer height. Value is 3.8 km.

Curves in Figs.3-a and 3-b represent calculated rain attenuation distributions. Calculated values agree well with measured values. As a result, it was found that the above-mentioned prediction method could be successfully applied to this second-phase experiment, which differed from the first-phase experiment in location, weather conditions and frequencies.

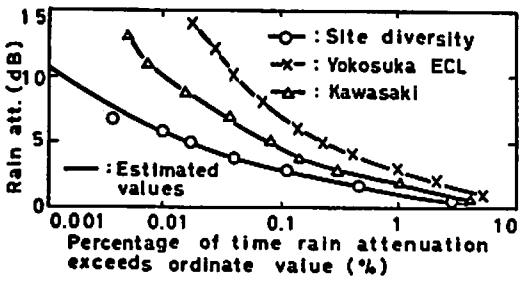

Fig.4 Site diversity effect at 55° elevation angle

3.3 Site diversity effects

Figure 4 shows rain attenuation distribution in site diversity operation at 55° elevation angle. Attenuation distributions at single sites are also shown. These data are obtained for 17 GHz attenuation at Yokosuka ECL and 18 GHz attenuation at 55° elevation angle within the time interval when the sun elevation angle is from 30° to 60°. A site diversity effects prediction method, based on the log-normal characteristics, was also proposed by Morita and Higuti.(2) The solid line in Fig.4 represents calculated values by this prediction method. Though rain attenuation distributions at Yokosuka and Kawasaki are not equal, the difference effect on the site diversity effect is very small. Therefore, the rain rate distribution at Yokosuka ECL is used for the calculation. As shown in Fig.4, calculated and measured values are in good agreement. Therefore, the prediction method for site diversity effects was mostly substantiated experimentally.

4. Conclusion

From these experimental results, a prediction method for rain attenuation distribution and site diversity effects, which was proposed by Morita and Higuti, is experimentally substantiated.

Acknowledgement The authors wish to thank Dr.M.Shimba, Mr.M.Shinji and Dr. K.Morita for their helpful suggestions and discussions.

References

(1) P.G.Davies, Proc. IEE, 123, 8 (Aug. 1976)

(2) K.Morita and I.Higuti, Trans. IECE Japan, E61, 6 (June 1978)